© 2016. Published by The Company of Biologists Ltd | Development (2016) 143, 1948-1957 doi:10.1242/dev.131953

RESEARCH ARTICLE

Fear-of-intimacy-mediated zinc transport controls the function of zinc-finger transcription factors involved in myogenesis

Marta Carrasco-Rando[1], Alexandra Atienza-Manuel[1], Paloma Martín[1], Richard Burke[2] and Mar Ruiz-Gómez[1,*]

ABSTRACT

Zinc is a component of one-tenth of all human proteins. Its cellular concentration is tightly regulated because its dyshomeostasis has catastrophic health consequences. Two families of zinc transporters control zinc homeostasis in organisms, but there is little information about their specific developmental roles. We show that the ZIP transporter Fear-of-intimacy (Foi) is necessary for the formation of *Drosophila* muscles. In *foi* mutants, myoblasts segregate normally, but their specification is affected, leading to the formation of a misshapen muscle pattern and distorted midgut. The observed phenotypes could be ascribed to the inactivation of specific zinc-finger transcription factors (ZFTFs), supporting the hypothesis that they are a consequence of intracellular depletion of zinc. Accordingly, *foi* phenotypes can be rescued by mesodermal expression of other ZIP members with similar subcellular localization. We propose that Foi acts mostly as a transporter to regulate zinc intracellular homeostasis, thereby impacting on the activity of ZFTFs that control specific developmental processes. Our results additionally suggest a possible explanation for the presence of large numbers of zinc transporters in organisms based on differences in ion transport specificity and/or degrees of activity among transporters.

KEY WORDS: Fear-of-intimacy, ZIP transporters, Mesoderm development, Zinc-finger transcription factors, *Drosophila*

INTRODUCTION

In a *Drosophila* genetic screen performed to identify novel genes required for myoblast specification and differentiation, we isolated two new alleles of *fear-of-intimacy* (*foi*), a gene that has been implicated in the processes of gonad and trachea morphogenesis and glial cell migration (Mathews et al., 2006; Pielage et al., 2004; Van Doren et al., 2003). *foi* encodes a protein of the ZIP (Zrt/IRT-like or solute carrier 39A, SLC39A) family of ion transporters (related to the vertebrate LIV-1 subfamily) that has specificity for zinc and localizes to the basolateral cell membrane (Lye et al., 2013; Mathews et al., 2005). Members of the ZIP family import zinc into the cytoplasm from either the extracellular space or intracellular organelles, and, together with the members of the zinc transporter (ZnT) family [also known as the cation diffusion facilitator family (CDF) or SLC30A], which remove zinc from the cytoplasm, control cellular zinc homeostasis. This control is very important because zinc is essential for animal life and it is a structural component of up to 10% of all human proteins (Andreini et al., 2006b). Accordingly, both zinc deficiency and excess cause clinical symptoms in humans, indicating that zinc cellular content has to be tightly regulated (Chasapis et al., 2012). Indeed, there are a large number of genes belonging to the ZIP and ZnT families encoded in mammalian and *Drosophila* genomes. Recently, functional analyses measuring the phenotypic effects of zinc toxicity in the fly have demonstrated that most of the 17 putative zinc transporters of *Drosophila* work as such and suggest that several of them could be acting together in the same tissue (Lye et al., 2012). However, in spite of the implication that several mammalian and *Drosophila* zinc transporters have roles in sustaining proper development and preventing disease, little is known about how they actually work at the cellular level and to what an extent they can substitute for each other. Here, we report that, in addition to its previously described requirements, Foi also has an essential role in muscle organogenesis. It impacts on several aspects of myogenesis, including the correct specification and differentiation of founder cells (FCs) and fusion-competent myoblasts (FCMs) in both somatic and visceral mesoderms. Thus, in *foi* mutants the FCMs segregate but cannot fully differentiate and remain as an immature population. The naïve myoblasts fail to fuse to FCs, do not contribute to mature muscles, and die during embryonic stage 14. Moreover, although FCs segregate and express a wide range of muscle identity genes, they are not correctly specified, as suggested by the aberrant muscle pattern observed in late embryos and its lack of innervation. Finally, the morphogenesis of the midgut is compromised by a failure in the formation or positioning of the midgut constrictions. In the latter case, the defects can be associated with modifications in the expression in the visceral mesoderm (VM) of several genes that control midgut morphogenesis. Interestingly, our evidence suggests that all phenotypes observed in *foi* mutants result from the inability of several zinc transcriptional regulators to function properly. This indicates that in the mesoderm *foi* functions as an essential zinc transporter, providing the intracellular zinc required for the activity of these proteins. Furthermore, the ability of other ZIP proteins to partially rescue *foi* mutant phenotypes when expressed in the mesoderm reinforces this interpretation. Indeed, it suggests that Foi specificity is a result not only of it being the only mesodermal ZIP member located in the basolateral plasma membrane, but also of its unique characteristics as zinc transporter, such as its affinity for zinc and its degree of activity. Similar to Foi, other zinc transporters required for early development both in vertebrates and invertebrates might impact on the function of developmentally important ZNTFs through regulation of intracellular zinc homeostasis.

RESULTS

Foi is required during embryonic myogenesis for the proper formation of somatic and visceral muscles

We isolated, in a genetic screen designed to identify novel genes involved in *Drosophila* myogenesis, two new alleles of *fear-of-intimacy* (*foi*), a gene encoding a zinc transporter of the ZIP family, which contains an N-terminal signal sequence, six transmembrane

[1]Centro de Biología Molecular Severo Ochoa, CSIC and UAM, C/Nicolás Cabrera 1, Madrid 28049, Spain. [2]School of Biological Sciences, Monash University, Wellington Road, Clayton, Victoria 3800, Australia.

*Author for correspondence (mruiz@cbm.csic.es)

M.R.-G., 0000-0002-9024-1400

Received 14 October 2015; Accepted 31 March 2016

Development (2016) 143, 1948-1957 doi:10.1242/dev.131953

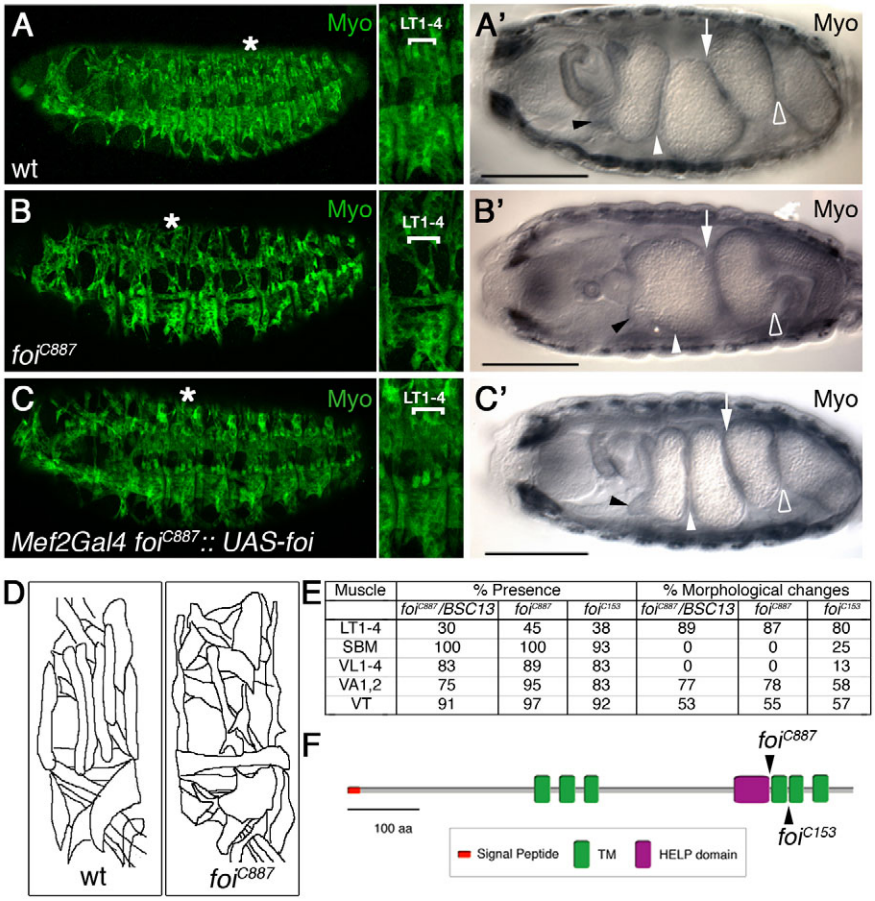

Muscle	% Presence			% Morphological changes		
	foi^{C887}/BSC13	foi^{C887}	foi^{C153}	foi^{C887}/BSC13	foi^{C887}	foi^{C153}
LT1-4	30	45	38	89	87	80
SBM	100	100	93	0	0	25
VL1-4	83	89	83	0	0	13
VA1,2	75	95	83	77	78	58
VT	91	97	92	53	55	57

Fig. 1. Mesodermal phenotypes of *foi* mutant embryos. Anti-Myosin (Myo) staining of stage 16 wild-type (wt; A), foi^{C887} (B) and *UAS-foi*/+; *Mef2-Gal4* foi^{C887}/foi^{C887} (C) embryos. (A-C) Lateral views showing the somatic muscle patterns in these genotypes. *foi* mutants have an aberrant muscle pattern with many absences and morphological changes. The position of LT muscles is indicated in the magnifications, which correspond to the hemisegments marked with an asterisk. (A′-C′) Ventral views of stage 16 embryos focussing on the visceral mesoderm. Note the absence of the first constriction (white arrowhead), the misplacement of the second constriction (white arrow) and the defective formation of the third constriction (unfilled arrowhead) in *foi* mutants, as well as the presence of the gastric caeca in wild-type and *foi*-rescued embryos and their absence in *foi* mutants (black arrowheads). (D) Camera lucida drawings of the muscle patterns depicted in the magnifications of panels A and B. (E) Table describing the muscle phenotypes for different *foi* mutant backgrounds where 'presence' indicates that a muscle appears in the experimental embryos at the position normally occupied by the wild-type muscle and 'morphological changes' refers to changes in shape or orientation. For quantification of phenotypes, 30 (foi^{C887}/*BSC13*), 33 (foi^{C887}) and 36 (foi^{C153}) abdominal hemisegments were scored. (F) Schematic of Foi protein domains. The position of the stop codons associated with the foi^{C887} and foi^{C153} alleles is indicated. In all figures, unless otherwise mentioned, anterior is to the left and ventral to the bottom. Panels A-C show *z* projections of several consecutive confocal sections. The rescue experiments were performed at 25°C. Scale bars: 100 µm.

domains and a HELP domain (Fig. 1F). Although it is known that *foi* participates in gonad formation, tracheal branch fusion and glial cell migration (Mathews et al., 2006; Pielage et al., 2004; Van Doren et al., 2003), its requirement for myogenesis has not been investigated in depth. The expression of Myosin in foi^{C887} and foi^{C153} mutant embryos showed a defective muscle pattern with missing muscles, morphological defects in dorsal, lateral and ventral groups of muscles, and a fusion defect, visualized by the reduced size of the remaining muscles (Fig. 1B,D,E, compare with Fig. 1A,A′,D; see also Fig. 4B,F and Fig. S1). The VM was also affected, as indicated by the absence of the gastric caeca and the anterior gut constriction (100% of cases; Fig. 1B′, black and white arrowheads), a misplacement of the middle constriction (100% of cases; Fig. 1B′, arrow), and a delay in the formation or failure in the completion of the posterior gut constriction (76% of cases; Fig. 1B′, unfilled arrowhead). Molecular analyses of both alleles showed transitions from C to T in the *foi* cDNA sequence that introduced premature stop codons at positions 2503 (foi^{C887}) and 2614 (foi^{C153}). These truncated the protein after the fourth and fifth transmembrane domains, respectively (Fig. 1F). We discarded the possibility that the mesodermal phenotypes of both mutants could be due to additional lesions, as we fully rescued them by reintroducing *foi* in the mesoderm using *Mef2-Gal4* (Fig. 1C,C′; data not shown). Moreover, we found that the basal expression of *foi* in a different *UAS-foi* line was sufficient to rescue *foi* mutants to adulthood, suggesting that low levels of Foi suffice to sustain its function.

Foi is necessary for the correct specification of FCMs and for implementing FC fates

Because the muscle defects in *foi* mutants affect all muscle groups (Fig. 1B,E) and *foi* is expressed both in FCs and FCMs (Fig. S3A,A′), we proceeded to analyse whether the two major myoblast populations were properly segregated and specified in these mutants. Using the enhancer trap line *rP298-LacZ*, which labels all muscle progenitors and founders (Nose et al., 1998; Ruiz-Gomez et al., 2000), we found that *foi* is not required for FC segregation (Fig. 2A,B). Furthermore, the expression in FCs and muscles of numerous muscle identity genes and markers, including *Krüppel* (*Kr*; Ruiz-Gomez et al., 1997), *eyes absent* (*eya*; Liu et al., 2009), *Connectin* (*Con*; Nose et al., 1992), *even skipped* (*eve*; Carmena et al., 1998), *vestigial* (*vg*; Williams et al., 1991), *lateral muscles scarcer* (*lms*; Müller et al., 2010), *slouch* (*slou*; also known as S59; Carmena et al., 1995) and *caupolican* (*caup*; Carrasco-Rando et al., 2011), showed the same FC identity code in foi^{C887} mutant embryos as in the wild type (Fig. 2C,D; Fig. S2). Hence, FCs appeared to be born with the correct muscle identity code. This suggests that the mutant *foi* phenotype was mainly due to a faulty implementation of their subsequent unique differentiation programmes. In the case of the FCM population, we found that the expression of two early markers specific for these myoblasts, *sticks and stones* (*sns*; Bour et al., 2000) and *hairy* (*h*; Martin et al., 2001; Ruiz-Gomez et al., 2002), was altered in foi^{C887} embryos. Thus, we failed to detect Hairy (Fig. 2E,F) and found a strong reduction in *sns* expression (Fig. 2G,H) in somatic FCMs, suggesting a failed specification and/or segregation of these myoblasts.

To distinguish between these alternatives, we analysed the expression of the FCM determinant *myoblast incompetent* [*minc*; also known as *lameduck* (*lmd*) and *gleeful* (*gfl*); Duan et al., 2001; Furlong et al., 2001; Ruiz-Gomez et al., 2002] in foi^{C887} embryos. *minc* was correctly expressed in these mutants (Fig. 2I,J), which indicated that the segregation of FCMs from FCs takes place

Development (2016) 143, 1948-1957 doi:10.1242/dev.131953

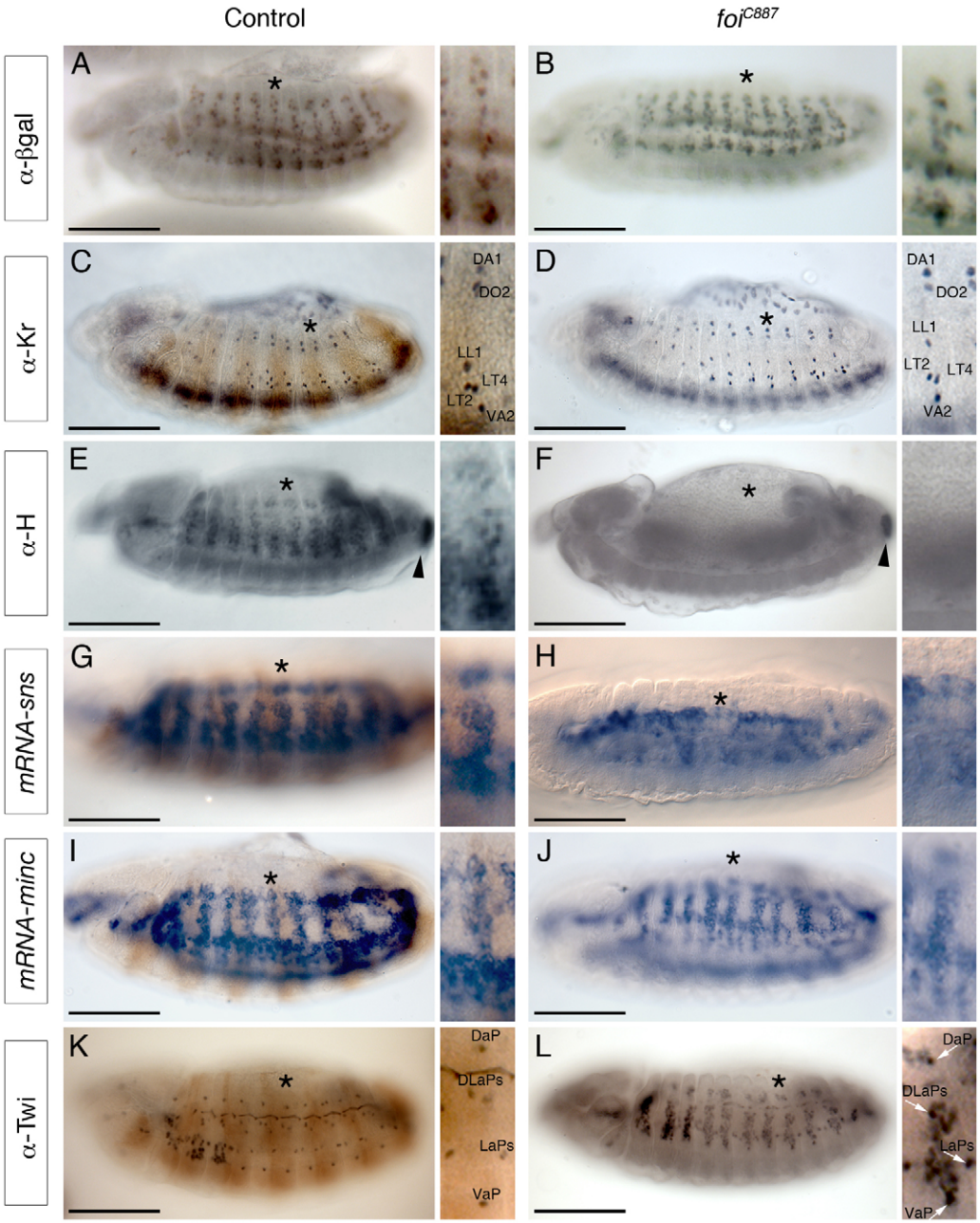

Fig. 2. The specification, but not the segregation, of FCs and FCMs is affected in *foi* mutants. Lateral views of stage 13-14 control (foi^{C887}/*TM3elav-lacZ* in C,G-K; *rP298* in A; Oregon R in E; left column) and foi^{C887} embryos (right column) stained for antibodies for different FCs or FCMs markers. The magnifications show the hemisegment marked by an asterisk in the corresponding embryo. Note that neither the segregation of FCs labelled by anti-β-galactosidase (A,B) nor the early expression of Kr in FCs (C,D) is affected in *foi* mutants. (E-J) Although FCMs segregate and express *minc* correctly in *foi* mutants (I,J) the expression of its downstream targets is abolished (H; compare E and F, the arrowheads indicate normal expression of H at the anal plate in *foi* mutants) or strongly reduced (*sns*; compare G and H) indicating their faulty specification. (K,L) At stage 13, the expression of Twi is restricted to the adult precursors in control embryos whereas in *foi* mutants is maintained in many unspecified FCMs. Scale bars: 100 µm.

normally. Hence, *foi* appeared to be required for FCM specification. To verify further that in the absence of Foi the segregated FCMs were incorrectly specified and did not initiate their early differentiation programme, we looked at the expression of Twist (Twi), a marker of mesodermal cells that is downregulated upon differentiation (Baylies and Bate, 1996; Ruiz-Gomez et al., 2002). We found that at stage 13 foi^{C887} FCMs still expressed high levels of Twi (Fig. 2K,L). Moreover, these undifferentiated FCMs were fated to die, as revealed by an antibody to activated Caspase 3 (Fig. S3C,D). The faulty specification of FCMs was not due to premature apoptosis, because blocking programmed cell death in *foi* embryos did not modify the *foi* phenotype, as revealed by ectopic Twi accumulation in FCMs (Fig. S3E,F).

The requirement for *foi* in the mesoderm was analysed further by assaying the ability of *UAS-foi* to rescue *foi* phenotypes. We first verified that pan-mesodermal overexpression of *foi* (*Mef2-Gal4*) did not modify the muscle pattern (not shown). As a control in our rescue experiments, we used foi^{C887} embryos carrying the *UAS-foi* transgene without a driver (Fig. 3A). Expressing *foi* in the whole mesoderm (*Mef2-Gal4*) or only in FCMs (*sns-Gal4*) fully (Fig. 3B;

Development (2016) 143, 1948-1957 doi:10.1242/dev.131953

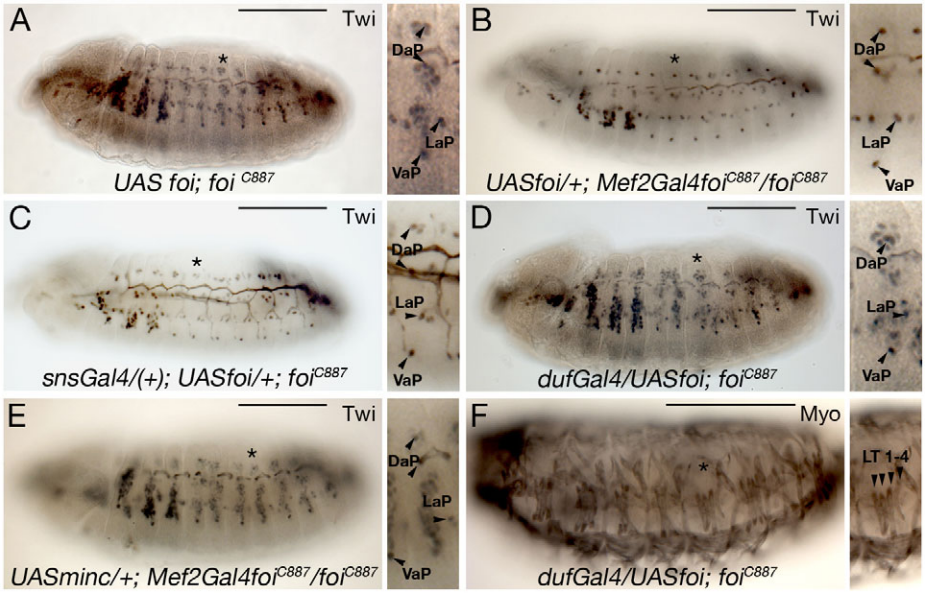

Fig. 3. *foi* is required in both FCs and FCMs. (A-D) Anti-Twist staining of stage 14 *UAS-foi*; foi^{C887} (A) and foi^{C887}-rescued embryos expressing *UAS-foi* with different mesodermal drivers. Both *Mef2-Gal4* and *sns-Gal4* produced a complete (B) or partial (C) rescue of FCM faulty specification, as observed by Twist expression, whereas the reintroduction of *UAS-foi* only in FCs failed to rescue the FCM phenotype of *foi* mutants (D). (E) Anti-Twi staining of a stage 14 foi^{C887} mutant embryo expressing *UAS-minc* in the mesoderm shows that overexpression of *minc* cannot replace the absence of *foi*. (F) Anti-Myosin staining of a stage 16 *duf-Gal4*/*UAS-foi*; foi^{C887}-rescued embryo showing that *foi* expression exclusively in FCs rescues the defects in muscle patterning, as revealed by the presence of LT muscles, tips of which are marked with arrowheads in the magnification. In A-F, the enlargements show details of the segment indicated by an asterisk in the corresponding embryos; in A-E the arrowheads point to the adult muscle precursors that accumulate higher levels of Twi and in F to the tips of the lateral muscles (LTs). In panels A,B,D-F images are composites of two/three focal planes. Rescues were performed at 29°C with the exception of the one shown in B, which was made at 25°C. Scale bars: 100 µm.

Fig. 4C,F) or almost completely (Fig. 3C; Fig. 4E,F) rescued the *foi* mutant phenotype, as revealed by Twi expression (Fig. 3; Fig. S1B) and number of Eve-expressing nuclei in muscle DA1 (Fig. 4). By contrast, expressing *foi* exclusively in founders (*duf-Gal4*) did not rescue the lack of FCM differentiation (Fig. 3D; Fig. 4D,F). However, *foi* expression in FCs corrected the defects in muscle patterning, as revealed by the presence of LT muscles in late embryos (Fig. 3F, compare with Fig. 1B,D). It is worth noting that the sole presence of the *UAS-foi* transgene was enough to reduce the loss-of-function (LOF) phenotype of *foi* in FCMs as revealed by Twi expression (compare the continuous distribution of Twi-positive cells in the latero-ventral region in Fig. 2L with the presence of two discrete clusters of Twi-positive cells in Fig. 3A and Fig. S1B) and could contribute to the partial recovery of the fusion phenotype observed in the *duf-Gal4* rescues (Figs 3 and 4). These results showed that *foi* is required in both myoblast populations to achieve the wild-type muscle pattern.

The function of Foi as a zinc transporter mediates its role in the mesoderm

Foi is a zinc transporter of the ZIP family, related to mammalian LIV-1 (SLC39A6) (Mathews et al., 2005). Thus, the *foi* phenotypes might be due to a depletion of intracellular zinc that impairs functioning of ZFTFs. A candidate protein to mediate the effect of Foi in FCMs is Minc, a ZFTF that regulates a common programme of FCMs differentiation. Hence, the expression of Minc target genes *sns* and *h* (Busser et al., 2012; Cunha et al., 2010) is severely affected in *foi* mutants. This effect is not rescued by pan-mesodermal overexpression of *minc* (Fig. 3E; Fig. S3B; data not shown), confirming that it is the activity of Minc and not its abundance that is compromised in *foi* mutants. Incorrect function of Minc could be caused by a requirement of Foi to translocate Minc to the nucleus. In fact, it has been shown that zebrafish Liv1 (Slc39a6 – Zebrafish Information Network) promotes the nuclear localization of Snail during epithelial-to-mesenchymal transition (Yamashita et al., 2004). We found that the subcellular localization of Minc was not affected in *foi* mutants (Fig. S4A,B), which suggested that the inability of Minc to regulate its targets does indeed arise from an intracellular drop in zinc concentration. This interpretation would also help explain the defects of muscle patterning seen in *foi* mutant embryos if other ZFTFs, such as Kr, were also ineffective. The only known direct target of *Kr* in the mesoderm is *knockout* (*ko*), a gene required for the innervation of ventral longitudinal muscles (VLMs) by RP motoneurons (Hartmann et al., 1997). We reasoned that if Kr fails to activate *ko*, VLMs in *foi* mutants should show innervation defects similar to *ko* embryos. Indeed (Fig. S4C-D′), in *foi* embryos the nerve branch segmental nerve b (SNb), which innervates the ventral muscles, did not defasciculate from the intersegmental nerve (ISN) (Fig. S4C,D, arrowheads), indicating that, similar to *ko* embryos, VLMs are not being recognised as target muscles by RP motoneurons.

Could a depletion of intracellular zinc also explain the phenotypes observed in the VM? To answer this question, we analysed in detail the patterns of expression of genes known to be essential for the correct patterning of the midgut. Because a role of Foi in regulating intracellular zinc homeostasis would affect preferentially those proteins requiring zinc for its activity, we focussed on ZFTFs as candidate factors to be responsible for the midgut defects observed in *foi* embryos. In the VM, Opa is expressed at the location of the first and third constrictions (Fig. 5A,B), neither of which is formed in *opa* mutants. In addition, Opa is also required for the expression of Scr in the

Development (2016) 143, 1948-1957 doi:10.1242/dev.131953

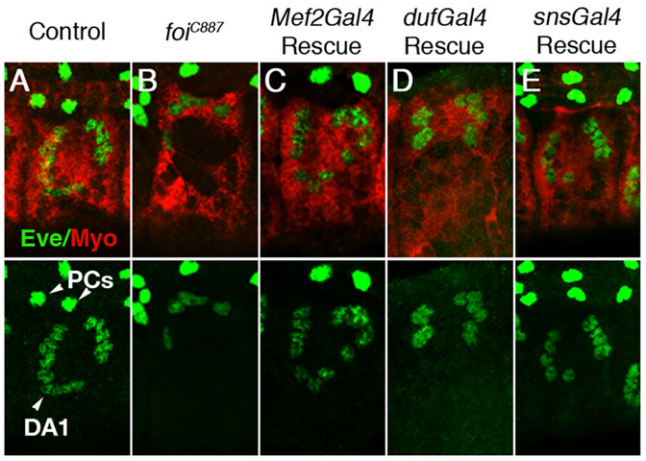

F

genotype	stage	DA1nuclei
Control *foi* ^{C887}/*TM3*	16	12.4± 0.4 (n=55)
foi ^{C887}	16	5.1± 0.5 (n=59)
Mef2Gal4 Rescue	16	11.5± 0.3 (n=32)
dufGal4 Rescue	16	9.2± 0.9 (n=45)
snsGal4 Rescue	16	11.4± 0.6 (n=34)

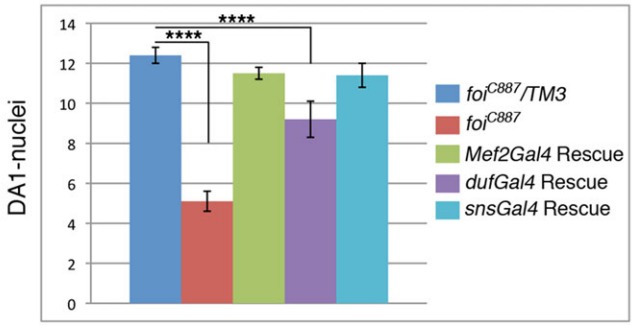

Fig. 4. Rescue of the fusion defects in *foi* mutant embryos providing *foi* in different mesodermal populations. (A-E) High magnification views of representative DA1 muscles stained with anti-Myosin and anti-Eve in stage 16 control (*foi*^{C887}/TM3; A), *foi*^{C887} (B) and *foi*^{C887}-rescued embryos using the following mesodermal drivers: *Mef2-Gal4* (C), *duf-Gal4* (D) and *sns-Gal4* (E). The genotypes of the rescued embryos correspond to the ones indicated in Fig. 3. PCs, pericardial cells. (F) Table and graphic showing the number of *eve*-expressing nuclei in DA1 muscles of embryos of the indicated genotypes (*n*, number of hemisegments quantified). Error bars indicate confidence intervals. ****P<0.0001 (one-way ANOVA). Panels A-E show *z* projections of several consecutive confocal sections.

anterior midgut and therefore for the development of the gastric caeca (Cimbora and Sakonju, 1995). We found that although *opa* expression was normal in *foi* mutants (Fig. 5C,D), Opa failed to activate Scr (Fig. 5E,F), thus explaining the absence of the gastric caeca observed in *foi* mutants. By contrast, the lack of the first constriction could not be ascribed to the controversial effect of Opa on Antp expression (Cimbora and Sakonju, 1995; Tremml and Bienz, 1989) (Fig. 5B), and might therefore be due to the inability of Opa to activate putative downstream targets acting at this position, or alternatively, depend on a different ZFTF. One such ZFTF could be Spalt major (Salm), which is required for the formation of the first midgut constriction (Fig. 5G,H). Its expression does not change in *foi* mutants (Fig. 5I,J), but its activity could not be tested because its targets in the VM are unknown.

foi mutants also show a posterior displacement of the middle constriction, which normally forms between parasegments (PS) 7 and 8 (Fig. 5A,B). This phenotype is fully penetrant and correlates with a shift of the posterior margin of the domain of expression of Ubx in the VM, so that it overlaps by four or five cells with the domains of expression of *wg* and *tsh* (Fig. 5K,L and brackets in K′,L′). Because Tsh has been shown to be involved in Wg-mediated repression of Ubx in the VM (Waltzer et al., 2001), we interpret this phenotype as a failure of the ZFTF Tsh to restrict Ubx expression normally. In these mutant embryos, the constriction still forms at the apposition of Ubx and AbdA domains of expression that now lies in the middle of PS 8 (Fig. 5B). Interestingly, in addition to the posterior expansion of Ubx expression we also observed a patch of four or five cells located posterior to the normal region of expression of Wg at PS 8 that ectopically co-expresses both *wg* and *tsh* (Fig. 5L′, asterisks). Because the activation of *wg* in the VM requires both AbdA and Dpp (Immerglück et al., 1990; Reuter et al., 1990), we decided to check whether *dpp* expression was also modified in *foi* mutants. As expected, we found an ectopic patch of *dpp* expression at PS 9 coinciding with the extra stripe of *wg* and *tsh* (Fig. 5M,N,N′). This patch appeared in the posterior domain of expression of *opa* in the VM. Therefore, it seemed likely that its presence could also reflect a failure of Opa to directly or indirectly repress *dpp*. Accordingly, we assayed the expression of *dpp* in *opa* mutants and found that it was also ectopically expressed in a patch of cells at PS 9 (Fig. 5O,O′). Because the third midgut constriction normally forms at this position and it is missing in both *opa* and *foi* mutants, it is possible that the ectopic patch of *dpp* expression might be responsible for the lack of this constriction. This interpretation is reinforced by the fact that ectopic expression of *dpp* throughout the VM suppresses the formation of the posterior midgut constriction (Staehling-Hampton and Hoffmann, 1994).

foi mutant phenotypes in the mesoderm are rescued by some other *Drosophila* ZIP transporters

Previous work has shown that Foi acts as an ion transporter specific for zinc that localizes to the basolateral outer membrane of the cells (Lye et al., 2013; Mathews et al., 2005). If its sole or main function in mesoderm development is to allow zinc influx into the cytosol, Foi might be replaced by other zinc transporters of the ZIP family with similar subcellular distributions. ZIP transporters with different subcellular localizations, or zinc transporters of the ZnT family, which act in the opposite direction and deplete the cytoplasmic supply of zinc, would probably not replace Foi. However, if in the mesoderm Foi's role is unrelated to its function as a regulator of zinc homeostasis, as previously suggested for Foi in controlling glial cell migration (Pielage et al., 2004), none of the known *Drosophila* zinc transporters should rescue the absence of *foi*.

Recently, 17 *Drosophila* genes encoding proteins with sequence homology to mammalian ZIP and ZnT families of zinc transporters have been identified and the proposed functions for several of them as transporters involved in zinc uptake or export have been validated (Lye et al., 2012, 2013). For our rescue experiments, we chose to use Catecholamines up (Catsup) as a representative of a ZIP transporter with organelle localization, ZnT1 (ZnT63C – FlyBase) as a ZnT transporter localized to the apical and basolateral plasma membranes, and ZIP42C.1 (encoded by *CG9428*) and ZIP71B (encoded by *CG10006*) as ZIP transporters localized both intracellularly and at the basolateral membrane (Lye et al., 2013). Using *Mef2-Gal4* to drive their pan-mesodermal expression, we found that neither ZnT1 (Fig. 6A) nor Catsup (Fig. 6B) rescued the

Development (2016) 143, 1948-1957 doi:10.1242/dev.131953

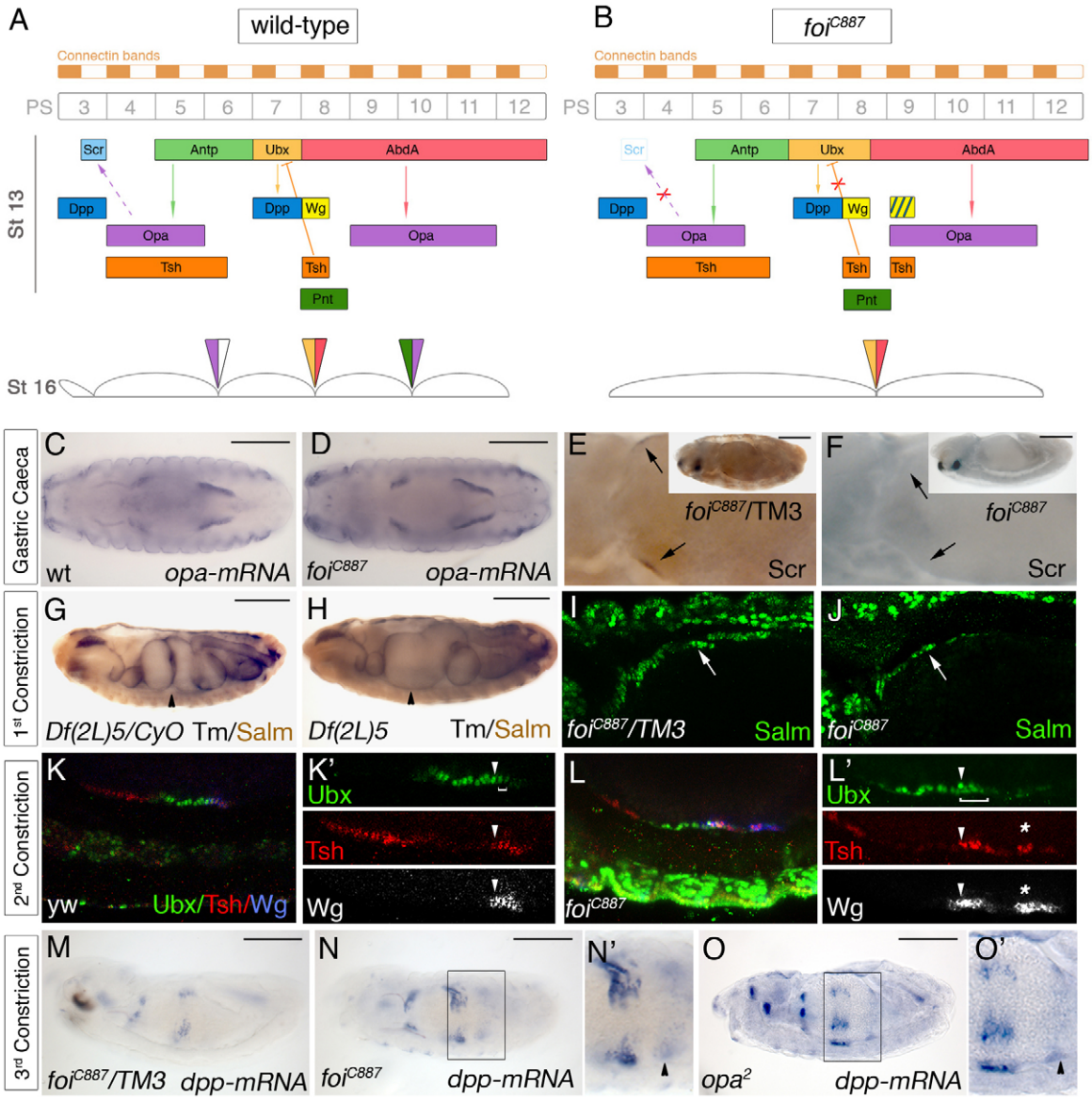

Fig. 5. *foi* phenotypes in the VM revealed the malfunction of ZFTFs relevant for midgut morphogenesis. (A,B) Schemes representing the regulatory genetic networks that drive the formation of the gastric caeca and the midgut chambers in wild-type (A) and in *foi* mutant (B) embryos. The upper bars display the position of Connectin stripes 2 to 11 and parasegments (PS) 3 to 12, below which the regions of expression of the relevant genes and regulatory interactions operating at stage 13 are depicted. The diagrams at the bottom show the compartmentation of the midgut as visualized at stage 16; the colour of the arrowheads indicates the borders of gene expression at which the constrictions form. (C,D) Ventral views of stage 14 wild-type (wt; C) and foi^{C887} (D) embryos hybridized with *opa* riboprobes. (E,F) Lateral views of the anterior midgut of stage 14 control (E) and foi^{C887} (F) embryos stained with anti-Scr. No Scr is seen in foi^{C887} (black arrows in F; compare with E). Insets show views of whole embryos. (G,H) Anti-Tropomyosin staining of stage 16 control (G) and *Df(2L)5* (H) embryos showing the absence of the anterior midgut constriction in *salm*/*salr*-deficient embryos. The arrowheads mark the normal position of this constriction. (I,J) Lateral views of stage 14 control (I) and foi^{C887} (J) embryos stained with anti-Salm. The arrows point to the anterior visceral mesoderm. (K-L′) Lateral views of stage 14 control *y w* (K,K′) and foi^{C887} (L,L′) embryos stained for Ubx (green), Tsh (Red) and Wg (blue in K,L, white in K′,L′) showing the expression of these proteins in the visceral mesoderm. The arrowheads in K′,L′ point to the intersection between Ubx and Tsh domains of expression; note that in control embryos only two cells beyond this position co-express Tsh and low levels of Ubx as a result of Tsh-mediated repression of Ubx (bracket in K′), whereas in *foi* mutants all Tsh- and Wg-expressing cells also co-express high levels of Ubx (bracket in L′). In addition, in foi^{C887} there is a patch of cells at PS 9 that ectopically co-express Tsh and Wg (asterisks in L′). (M-O′) Lateral views of stage 14 foi^{C887}/TM3 (M), foi^{C887} (N,N′) and opa^{2} (O,O′) embryos hybridized with *dpp* riboprobes. The black arrowheads in N′ and O′ point to a patch of ectopic expression of *dpp* at PS 9 (compare with M). N′ and O′ show high magnifications of the boxed areas in N and O, respectively. Scale bars: 100 µm.

foi mutant phenotype, whereas ZIP42C1 and ZIP71B substantially rescued it, as revealed by expression of *twi*, *sns* and Eve-expressing DA1 nuclei (Fig. 6D,E; Fig. S5; Fig. S1). We found, however, that ZIP71B induced fusion defects (visualized by the expression of Tm) not seen by pan-mesodermal expression of Foi or ZIP42C1 (Fig. 1C; Fig. 6F; Fig. S5). Curiously, human LIV-1 (SLC39A6 – Human Gene Nomenclature Database), closely related in sequence to Foi, did not rescue any of the *foi* phenotypes (Fig. 6C). Taken together, our results are in agreement with a role of Foi in regulating zinc homeostasis in the mesoderm.

DISCUSSION

Zinc is an essential ion in cells where it plays different roles, intervening in the metabolism of proteins, nucleic acids,

Development (2016) 143, 1948-1957 doi:10.1242/dev.131953

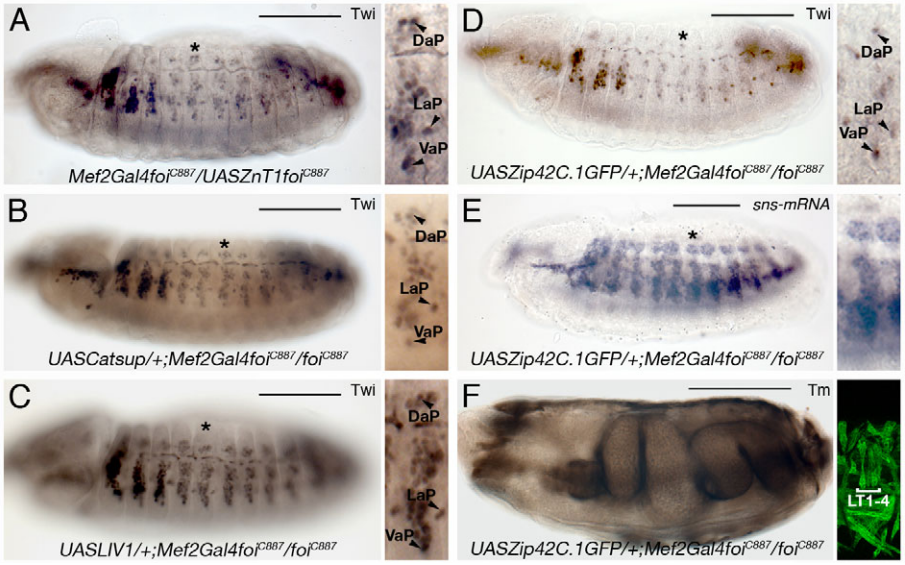

Fig. 6. Mesodermal rescues of *foi* phenotypes with different zinc transporters. (A-F) Lateral views of stage 14 (A-E) and ventral view of stage 16 (F) foi^{C887} embryos with pan-mesodermal expression of the zinc transporters *ZnT1* (A), *Catsup* (B), *LIV1* (C) and *Zip42C.1* (D-F). The segments indicated by asterisks in A-E are shown as close-ups. In F, the close-up shows a confocal section of an abdominal segment of an embryo of the same genotype stained with anti-Tm and positioned laterally to visualize the muscle pattern. Only *Zip42C.1* can rescue all the mesodermal phenotypes of *foi* as revealed by the expression of Twi (A-D; compare with Fig. 2K), *sns* (E; compare with Fig. 2G) and Tm (F; compare with Fig. 1A′-C′). Images in panels A,B are composites of two/three focal planes. Scale bars: 100 µm.

carbohydrates and lipids. After iron, zinc is the most abundant transition metal in living organisms being a component of ∼10% of all proteins. It acts as a co-factor of many cellular enzymes and is required for the structural stability and function of a large number of proteins, including ZnFTs, proteins bearing RING fingers and LIM domains, and zinc regulatory proteins such as metallothionein and matrix metalloproteinases (Andreini et al., 2006a). Therefore, zinc is required for most cellular functions where these proteins are involved, including defence against oxidative stress, response to DNA damage, cellular communication, transcriptional regulation and cell migration. Its concentration must be tightly regulated at the single-cell level to avoid the pernicious consequences associated with zinc deficiency, and the cellular toxicity of its excessive accumulation (reviewed by Chasapis et al., 2012). In normal cells, much of the intracellular zinc is found associated with proteins, there being a tight control of its homeostasis. Two large families of zinc transporters (the ZIP family, which imports zinc into the cytoplasm, and the ZnT family, which exports zinc out of the cytoplasm) comprise 24 members in mammals and 17 members in *Drosophila* (Lichten and Cousins, 2009; Lye et al., 2013). This is in striking contrast with the cellular control of copper homeostasis, which is accomplished by only four transporters (Gupta and Lutsenko, 2009), and therefore raises the question of why there is a need for so many transporters.

Data obtained from knockout mice for various ZIP and ZnT members (reviewed by Chasapis et al., 2012) and from a functional analysis of all the zinc transporters in *Drosophila* (Lye et al., 2012, 2013) have revealed that there are specific requirements for several zinc transporters and that this specificity relies, at least in part, on the patterns of expression of their encoding genes and on their subcellular localization. Interestingly, the function of some transporters is conserved across species (Wang et al., 2009). However, despite the considerable amount of studies that address the role of zinc transporters in organisms and the clear evidence indicating their crucial requirement during development, little is known about their specific developmental roles. Exceptions are the requirement of zebrafish Liv1 (also known as ZIP6) for the nuclear localization of Snail, essential for the epithelial-to-mesenchymal transition that drives gastrulation (Yamashita et al., 2004), and the requirement of *Catsup* for the normal trafficking of Notch (Groth et al., 2013).

Here, we have focussed on deciphering the specific developmental roles and mode of action of Foi, a *Drosophila* zinc transporter of the ZIP family that localizes to the basolateral surface of the plasma membrane and is highly specific for zinc (Lye et al., 2013; Mathews et al., 2005). It was already known that the zinc transport activity of Foi is essential for gonadal development (Mathews et al., 2006). Our data indicate that, in addition to its role in gonads, trachea and glial cells (Pielage et al., 2004; Van Doren et al., 2003), Foi is necessary for the normal development of somatic and visceral muscles. Although in *foi* mutants gastrulation is not affected and the different subtypes of somatic and visceral myoblasts segregate normally, these are not well specified. Thus, we find that even though FCMs express the master regulator of their fate, *minc*, which encodes a ZFTF, Minc does not activate *sns* and *h*, two of its effectors in FCMs. Therefore, FCMs remain undifferentiated (as revealed by their failure to repress *twi*) and unable to fuse, and will subsequently die. Cell death is likely to be a consequence of their faulty specification, because preventing FCM death does not modify the phenotype of *foi* loss of function. Similarly, despite the fact that FCs express the normal code of muscle-identity genes, the resulting muscles are abnormally specified, as indicated by their aberrant orientation, shape and innervation. These aspects of their abnormal identity are rescued by the reintroduction of *foi* only in founders, although this condition does not completely rescue the fusion defect. Finally, we also show that *foi* is necessary for the correct specification of the visceral mesoderm that drives the formation of the midgut constrictions. Because Foi is a zinc transporter of the ZIP family for which expression is enriched in the mesoderm, we anticipated that all the mesodermal phenotypes that we observed could result from an intracellular depletion of zinc. We reasoned that this shortage of zinc could affect the activity of zinc proteins and more specifically of ZFTFs. In agreement with our hypothesis, all the *foi* phenotypes that we have characterized in the mesoderm might in principle be ascribed to the functional failure of a ZFTF operating in the specific myoblast population being analysed. Thus, the FCM phenotype of *foi* mimics the *minc* LOF phenotype. The lack of innervation of the ventral muscles resembles the LOF of *ko*, a direct target of Kr in the mesoderm. The missing gastric caeca in *foi* mutant embryos might be a consequence of the failure of Opa to activate *Scr* in the visceral mesoderm. The posterior displacement of the middle constriction

Development (2016) 143, 1948-1957 doi:10.1242/dev.131953

coincides with the posterior expansion of the Ubx region of expression in the visceral mesoderm into the Tsh territory, indicating that Tsh is now unable to repress *Ubx*. Finally, the absence of the posterior midgut constriction might be due to the inability of Opa to repress *dpp*. In addition, although the putative targets of Salm, involved in the formation of the anterior midgut constriction remain unidentified, we tentatively propose that a malfunction of Salm might be responsible for the absence of this constriction in *foi* mutants. Interestingly, the nuclear localization of all ZFTFs tested, including Minc, Kr, Salm and Tsh, is not affected in *foi* mutants (Fig. S4; Fig. 2D; Fig. 4E,F). This is in contrast to the role of zebrafish Liv1, which is required for the nuclear translocation of Snail, and indicates that during mesodermal development it is the activity of ZFTFs and not their nuclear localization that is affected by the depletion of intracellular zinc.

Our results suggest that Foi helps maintain intracellular zinc homeostasis. Can this interpretation also explain the phenotypes of *foi* mutants in the gonads, trachea and glial cells? We have not addressed directly the requirement for *foi* in these tissues. However, it is worth noting that the disruption of fusion in lateral tracheal branches found in *foi* mutants is identical to that of *escargot* (*esg*) mutants (Samakovlis et al., 1996; Van Doren et al., 2003), and although Esg, a ZFTF, is normally expressed in the fusion tip cells (Van Doren et al., 2003), it might be unable to normally regulate Dysfusion expression in these cells (Jiang and Crews, 2003). Similarly, the defects of *foi* mutants in glia could be related to another ZFTF, Jing, for which the LOF phenotype in these cells (thinner longitudinal connectives and fused commissures) resembles that of *foi* (Pielage et al., 2004; Sun et al., 2006). Finally, both *foi* and the ZFTF *zfh1* have similar LOF phenotypes in gonads (Lai et al., 1993; Moore et al., 1998).

If, as our data suggest, Foi is solely acting as a zinc transporter, it follows that other zinc transporters of the same subfamily with similar cellular distributions should rescue *foi* LOF phenotypes. This is what we observed when we used ZIP42C1, closely related to mammalian ZIP1-3 (SLC39A1-3), and ZIP71B, very related to mammalian ZIP5 and ZIP6 (SLC39A5 and SLC39A6) and Foi (Lye et al., 2012), in our rescue experiments. Furthermore, this interpretation was reinforced by the worsening of phenotypes when we attempted rescuing the absence of Foi with ZnT1. Still, it should be stressed that none of the zinc transporters tested provided such a complete rescue as that obtained with Foi. In fact, although introduction of ZIP71B in the mesoderm recovered the expression of *sns*, *h* and *twi* to wild-type levels, its mesodermal overexpression induced a defect consistent with reduced fusion, which was more severe when the rescue experiments were performed at 29°C (Fig. S5). This defect was not observed when ZIP42C.1, which has a lesser sequence similarity to Foi than does ZIP71B, or Foi itself were used. An explanation for this difference could be that ZIP71B is very efficient in transporting zinc and might lead to mild zinc toxicity. In agreement with this interpretation, we detected a few apoptotic myoblasts in the embryos rescued with ZIP71B. However, we could not rescue any of the mesodermal *foi* phenotypes with mammalian LIV-1, a transporter closely related by sequence to Foi, which localizes to plasma membrane lamellipodiae. One possible explanation could be the previously reported low level of LIV-1 protein accumulation in *Drosophila* S2 cells (Taylor et al., 2003). Since in our assays we found substantial accumulation of LIV-1 RNA, the discrepancy between LIV-1 RNA and protein levels might be due to the proposed post-transcriptional regulation of LIV-1, which targets the protein to degradation by the ubiquitin proteasome pathway (Taylor et al., 2003). Alternatively, the failure to rescue *foi* phenotypes with LIV-1 could derive from its preferential accumulation in lamellipodia and/or its function in promoting the nuclear translocation of the ZFTF Snail, a function not shared by Foi.

In conclusion, we show that Foi, a zinc transporter of the ZIP family, plays an important role during development, being necessary for the correct specification and consequent differentiation of mesodermal derivatives. Our results strongly support the conclusion that in these processes Foi acts mostly or exclusively as a zinc transporter that regulates zinc cellular homeostasis. We also show that Foi function can be partially replaced by other transporters of the same family with similar subcellular localization. The fact that the rescue is not complete indicates that, besides the differences in pattern of expression and subcellular localization, the functional characteristics of the zinc transporters relative to ion transport specificity and/or transport activity contribute to their functional specificity. This may help explain why organisms maintain such large families of transporters to control zinc homeostasis.

MATERIALS AND METHODS

Drosophila strains

Flies were maintained under standard conditions at 25°C. The following stocks were used: *Oregon R*, *Df(3L)H99*, $foi^{l(3)j8E8}$ (Bloomington Stock Center); *Df(3L)*BSC13 [*Drosophila* Genomics and Genetic Resources (DGGR)]; foi^{C153}, foi^{C887} (this study); foi^{2633} (Van Doren et al., 2003); *rp298* (Nose et al., 1998); *Mef2-Gal4*, *duf-Gal4*, *sns-Gal4*, *UAS-minc* (Ruiz-Gomez et al., 2002); *UAS-ZnT1* (Wang et al., 2009); *UAS-Zip42C.1GFP* (Lye et al., 2013).

Molecular biology

To determine the DNA sequences of *foi* alleles, we sequenced PCR products amplified from genomic DNA extracted from homozygous mutant embryos that were selected for lack of GFP expression present in the balancer chromosome *TM3 twi-Gal4::2x UAS-eGFP*. To obtain *UAS-foi* and *UAS-Catsup* we subcloned the complete cDNAs recovered from the full-length EST clones RE41071 and LD23513 (DGRC) into the pUAST vector followed by transformation into *y w* embryos. *UAS-Zip71B* was obtained by PCR amplification using as template the full-length EST IP18018 clone (DGRC) and subcloning into *pUASt-attB* and *UAS-LIV1* (pTW-LIV1) was generated by Gateway cloning technology using the HsCD00289188 cDNA clone (DNASU Plasmid Repository, the ORFeome Collaboration). These two constructs were inserted at 22A by site-directed transformation. The constructs were verified by sequence analysis. All rescue experiments were carried out at 25°C and 29°C and unless otherwise indicated the results documented in the figures were obtained at 29°C.

In situ hybridization and immunohistochemistry

Whole-mount RNA *in situ* hybridizations with digoxigenin-labelled *dpp* cDNA (Padgett et al., 1987), LD30441, RE33150 and RE41071 (*opa*, *lms*, *foi* cDNAs, Berkeley *Drosophila* Genome Project) probes and immunocytochemistry were performed as described previously (Martín et al., 2001). The following primary antibodies were used: rabbit anti-β-Gal (1:5000; cat. no. 55976, Cappel), mouse anti-β-Gal (1:1000; cat. no. Z3781, Promega), rabbit anti-cleaved Caspase 3 (1:50; Asp175, cat. no. 9661, Cell Signaling Technology), rabbit anti-GFP (1:300; cat. no. A-6455, Molecular Probes), mouse anti-GFP (1:100; cat. no. 11814460001, Roche), mouse anti-Hairy (1:10; a gift from D. Ish-Horowicz, University College London, UK), guinea pig anti-Kr and anti-Eve (1:200 and 1:500, respectively; Kosman et al., 1998), rabbit anti-muscle Myosin (1:200; Kiehart and Feghali, 1986), rabbit anti-Salm (1:100; a gift from J. F. de Celis, CBMSO-CSIC, Madrid, Spain), rabbit S59 (recognises Slou; 1:50; Carmena et al., 1995), rabbit anti-Scr (1:100; Mahaffey and Kaufman, 1987), rat anti-Tm (1:100; MAC141, Babraham Bioscience Technologies), rabbit anti-Twi (1:1000; Roth et al., 1989), guinea pig anti-Tsh (1:1000; Peng et al., 2009), rabbit anti-Ubx (1:100; Agrawal et al., 2011), rat anti-Antp (1:500, gift from

M. Scott, Stanford University School of Medicine, Palo Alto, CA, USA), rat anti-Caup (1:50; Diez del Corral et al., 1999), mouse anti-Connectin (1:10; Meadows et al., 1994), guinea pig anti-Lmd (1:100; Duan et al., 2001), rabbit anti-Lamin (1:1000; Fisher et al., 1982), rabbit anti-Vg (1:500; Williams et al., 1991), mouse anti-Eya (Mab1046), anti-FasII (1D4) and anti-Wg (4D4) (1:1000, 1:5, and 1:50, respectively, Developmental Studies Hybridoma Bank). Images were obtained using a Zeiss Axiophot microscope and confocal microscopes LSM510 and LSM710 (Zeiss) and figures were processed using Adobe Photoshop CS4 and ImageJ software.

Acknowledgements
We thank J. Modolell, J. F. de Celis and S. Campuzano for critical reading of the manuscript. We are most grateful to the following colleagues for sharing the reagents used in this study: D. Kiehart, M. Van Doren, A. Nose, B. Zhou, R. Renkawitz-Pohl, D. Ish-Horowicz, D. Kosman, S. Roth, M. Scott, R. White, S. Carroll, H. Nguyen, P. Fisher and R. Mann. We also thank the Bloomington Stock Center, the Developmental Studies Hybridoma Bank, the *Drosophila* Genomics Resource Center and the DNASU plasmid repository for reagents; and E. Caminero and M. Casado from the *Drosophila* Transgenic Service of the CBMSO for their technical support.

Competing interests
The authors declare no competing or financial interests.

Author contributions
M.C.-R. performed experiments, analysed data and contributed to writing the manuscript; P.M. and A.A.-M. carried out experiments; R.B. contributed the UAS ZIP lines; M.R.-G. conceived the study, supervised the work, performed some experiments and wrote the manuscript.

Funding
This work is supported by grants from Ministerio de Economía y Competitividad [BFU2010-14884 and BFU2013-45430-P to M.R.-G.]. We also acknowledge institutional support from Fundación Ramón Areces to the Centro de Biología Molecular Severo Ochoa (CBMSO).

Supplementary information
Supplementary information available online at
http://dev.biologists.org/lookup/suppl/doi:10.1242/dev.131953/-/DC1

References
Agrawal, P., Habib, F., Yelagandula, R. and Shashidhara, L. S. (2011). Genome-level identification of targets of Hox protein Ultrabithorax in Drosophila: novel mechanisms for target selection. *Sci. Rep.* **1**, 205.
Andreini, C., Banci, L., Bertini, I. and Rosato, A. (2006a). Counting the zinc-proteins encoded in the human genome. *J. Proteome Res.* **5**, 196-201.
Andreini, C., Banci, L., Bertini, I. and Rosato, A. (2006b). Zinc through the three domains of life. *J. Proteome Res.* **5**, 3173-3178.
Baylies, M. K. and Bate, M. (1996). twist: a myogenic switch in Drosophila. *Science* **272**, 1481-1484.
Bour, B. A., Chakravarti, M., West, J. M. and Abmayr, S. M. (2000). Drosophila SNS, a member of the immunoglobulin superfamily that is essential for myoblast fusion. *Genes Dev.* **14**, 1498-1511.
Busser, B. W., Huang, D., Rogacki, K. R., Lane, E. A., Shokri, L., Ni, T., Gamble, C. E., Gisselbrecht, S. S., Zhu, J., Bulyk, M. L. et al. (2012). Integrative analysis of the zinc finger transcription factor Lame duck in the Drosophila myogenic gene regulatory network. *Proc. Natl. Acad. Sci. USA* **109**, 20768-20773.
Carmena, A., Bate, M. and Jimenez, F. (1995). Lethal of scute, a proneural gene, participates in the specification of muscle progenitors during Drosophila embryogenesis. *Genes Dev.* **9**, 2373-2383.
Carmena, A., Gisselbrecht, S., Harrison, J., Jimenez, F. and Michelson, A. M. (1998). Combinatorial signaling codes for the progressive determination of cell fates in the Drosophila embryonic mesoderm. *Genes Dev.* **12**, 3910-3922.
Carrasco-Rando, M., Tutor, A. S., Prieto-Sánchez, S., González-Pérez, E., Barrios, N., Letizia, A., Martín, P., Campuzano, S. and Ruiz-Gómez, M. (2011). Drosophila araucan and caupolican integrate intrinsic and signalling inputs for the acquisition by muscle progenitors of the lateral transverse fate. *PLoS Genet.* **7**, e1002186.
Chasapis, C. T., Loutsidou, A. C., Spiliopoulou, C. A. and Stefanidou, M. E. (2012). Zinc and human health: an update. *Arch. Toxicol.* **86**, 521-534.
Cimbora, D. M. and Sakonju, S. (1995). Drosophila midgut morphogenesis requires the function of the segmentation gene odd-paired. *Dev. Biol.* **169**, 580-595.
Cunha, P. M. F., Sandmann, T., Gustafson, E. H., Ciglar, L., Eichenlaub, M. P. and Furlong, E. E. M. (2010). Combinatorial binding leads to diverse regulatory responses: Lmd is a tissue-specific modulator of Mef2 activity. *PLoS Genet.* **6**, e1001014.
Diez del Corral, R., Aroca, P., Gomez-Skarmeta, J. L., Cavodeassi, F. and Modolell, J. (1999). The Iroquois homeodomain proteins are required to specify body wall identity in Drosophila. *Genes Dev.* **13**, 1754-1761.
Duan, H., Skeath, J. B. and Nguyen, H. T. (2001). Drosophila Lame duck, a novel member of the Gli superfamily, acts as a key regulator of myogenesis by controlling fusion-competent myoblast development. *Development* **128**, 4489-4500.
Fisher, P. A., Berrios, M. and Blobel, G. (1982). Isolation and characterization of a proteinaceous subnuclear fraction composed of nuclear matrix, peripheral lamina, and nuclear pore complexes from embryos of Drosophila melanogaster. *J. Cell Biol.* **92**, 674-686.
Furlong, E. E. M., Andersen, E. C., Null, B., White, K. P. and Scott, M. P. (2001). Patterns of gene expression during Drosophila mesoderm development. *Science* **293**, 1629-1633.
Groth, C., Sasamura, T., Khanna, M. R., Whitley, M. and Fortini, M. E. (2013). Protein trafficking abnormalities in Drosophila tissues with impaired activity of the ZIP7 zinc transporter Catsup. *Development* **140**, 3018-3027.
Gupta, A. and Lutsenko, S. (2009). Human copper transporters: mechanism, role in human diseases and therapeutic potential. *Future Med. Chem.* **1**, 1125-1142.
Hartmann, C., Landgraf, M., Bate, M. and Jackle, H. (1997). Kruppel target gene knockout participates in the proper innervation of a specific set of Drosophila larval muscles. *EMBO J.* **16**, 5299-5309.
Immerglück, K., Lawrence, P. A. and Bienz, M. (1990). Induction across germ layers in Drosophila mediated by a genetic cascade. *Cell* **62**, 261-268.
Jiang, L. and Crews, S. T. (2003). The Drosophila dysfusion basic helix-loop-helix (bHLH)-PAS gene controls tracheal fusion and levels of the trachealess bHLH-PAS protein. *Mol. Cell. Biol.* **23**, 5625-5637.
Kiehart, D. P. and Feghali, R. (1986). Cytoplasmic myosin from Drosophila melanogaster. *J. Cell Biol.* **103**, 1517-1525.
Kosman, D., Small, S. and Reinitz, J. (1998). Rapid preparation of a panel of polyclonal antibodies to Drosophila segmentation proteins. *Dev. Genes Evol.* **208**, 290-294.
Lai, Z. C., Rushton, E., Bate, M. and Rubin, G. M. (1993). Loss of function of the Drosophila zfh-1 gene results in abnormal development of mesodermally derived tissues. *Proc. Natl. Acad. Sci. USA* **90**, 4122-4126.
Lichten, L. A. and Cousins, R. J. (2009). Mammalian zinc transporters: nutritional and physiologic regulation. *Annu. Rev. Nutr.* **29**, 153-176.
Liu, Y.-H., Jakobsen, J. S., Valentin, G., Amarantos, I., Gilmour, D. T. and Furlong, E. E. M. (2009). A systematic analysis of Tinman function reveals Eya and JAK-STAT signaling as essential regulators of muscle development. *Dev. Cell* **16**, 280-291.
Lye, J. C., Richards, C. D., Dechen, K., Paterson, D., de Jonge, M. D., Howard, D. L., Warr, C. G. and Burke, R. (2012). Systematic functional characterization of putative zinc transport genes and identification of zinc toxicosis phenotypes in Drosophila melanogaster. *J. Exp. Biol.* **215**, 3254-3265.
Lye, J. C., Richards, C. D., Dechen, K., Warr, C. G. and Burke, R. (2013). In vivo zinc toxicity phenotypes provide a sensitized background that suggests zinc transport activities for most of the Drosophila Zip and ZnT genes. *J. Biol. Inorg. Chem.* **18**, 323-332.
Mahaffey, J. W. and Kaufman, T. C. (1987). Distribution of the Sex combs reduced gene products in Drosophila melanogaster. *Genetics* **117**, 51-60.
Martin, B. S., Ruiz-Gomez, M., Landgraf, M. and Bate, M. (2001). A distinct set of founders and fusion-competent myoblasts make visceral muscles in the Drosophila embryo. *Development* **128**, 3331-3338.
Mathews, W. R., Wang, F., Eide, D. J. and Van Doren, M. (2005). Drosophila fear of intimacy encodes a Zrt/IRT-like protein (ZIP) family zinc transporter functionally related to mammalian ZIP proteins. *J. Biol. Chem.* **280**, 787-795.
Mathews, W. R., Ong, D., Milutinovich, A. B. and Van Doren, M. (2006). Zinc transport activity of Fear of Intimacy is essential for proper gonad morphogenesis and DE-cadherin expression. *Development* **133**, 1143-1153.
Meadows, L. A., Gell, D., Broadie, K., Gould, A. P. and White, R. A. (1994). The cell adhesion molecule, connectin, and the development of the Drosophila neuromuscular system. *J. Cell Sci.* **107**, 321-328.
Moore, L. A., Broihier, H. T., Van Doren, M., Lunsford, L. B. and Lehmann, R. (1998). Identification of genes controlling germ cell migration and embryonic gonad formation in Drosophila. *Development* **125**, 667-678.
Müller, D., Jagla, T., Bodart, L. M., Jährling, N., Dodt, H.-U., Jagla, K. and Frasch, M. (2010). Regulation and functions of the lms homeobox gene during development of embryonic lateral transverse muscles and direct flight muscles in Drosophila. *PLoS ONE* **5**, e14323.
Nose, A., Mahajan, V. B. and Goodman, C. S. (1992). Connectin: a homophilic cell adhesion molecule expressed on a subset of muscles and the motoneurons that innervate them in Drosophila. *Cell* **70**, 553-567.
Nose, A., Isshiki, T. and Takeichi, M. (1998). Regional specification of muscle progenitors in Drosophila: the role of the msh homeobox gene. *Development* **125**, 215-223.

Development (2016) 143, 1948-1957 doi:10.1242/dev.131953

Padgett, R. W., St Johnston, R. D. and Gelbart, W. M. (1987). A transcript from a Drosophila pattern gene predicts a protein homologous to the transforming growth factor-beta family. *Nature* **325**, 81-84.

Peng, H. W., Slattery, M. and Mann, R. S. (2009). Transcription factor choice in the Hippo signaling pathway: homothorax and yorkie regulation of the microRNA bantam in the progenitor domain of the Drosophila eye imaginal disc. *Genes Dev.* **23**, 2307-2319.

Pielage, J., Kippert, A., Zhu, M. and Klämbt, C. (2004). The Drosophila transmembrane protein Fear-of-intimacy controls glial cell migration. *Dev. Biol.* **275**, 245-257.

Reuter, R., Panganiban, G. E., Hoffmann, F. M. and Scott, M. P. (1990). Homeotic genes regulate the spatial expression of putative growth factors in the visceral mesoderm of Drosophila embryos. *Development* **110**, 1031-1040.

Roth, S., Stein, D. and Nüsslein-Volhard, C. (1989). A gradient of nuclear localization of the dorsal protein determines dorsoventral pattern in the Drosophila embryo. *Cell* **59**, 1189-1202.

Ruiz-Gomez, M., Romani, S., Hartmann, C., Jackle, H. and Bate, M. (1997). Specific muscle identities are regulated by Kruppel during Drosophila embryogenesis. *Development* **124**, 3407-3414.

Ruiz-Gomez, M., Coutts, N., Price, A., Taylor, M. V. and Bate, M. (2000). Drosophila dumbfounded: a myoblast attractant essential for fusion. *Cell* **102**, 189-198.

Ruiz-Gomez, M., Coutts, N., Suster, M. L., Landgraf, M. and Bate, M. (2002). myoblasts incompetent encodes a zinc finger transcription factor required to specify fusion-competent myoblasts in Drosophila. *Development* **129**, 133-141.

Samakovlis, C., Hacohen, N., Manning, G., Sutherland, D. C., Guillemin, K. and Krasnow, M. A. (1996). Development of the Drosophila tracheal system occurs by a series of morphologically distinct but genetically coupled branching events. *Development* **122**, 1395-1407.

Staehling-Hampton, K. and Hoffmann, F. M. (1994). Ectopic decapentaplegic in the Drosophila midgut alters the expression of five homeotic genes, dpp, and wingless, causing specific morphological defects. *Dev. Biol.* **164**, 502-512.

Sun, X., Morozova, T. and Sonnenfeld, M. (2006). Glial and neuronal functions of the Drosophila homolog of the human SWI/SNF gene ATR-X (DATR-X) and the jing zinc-finger gene specify the lateral positioning of longitudinal glia and axons. *Genetics* **173**, 1397-1415.

Taylor, K. M., Morgan, H. E., Johnson, A., Hadley, L. J. and Nicholson, R. I. (2003). Structure-function analysis of LIV-1, the breast cancer-associated protein that belongs to a new subfamily of zinc transporters. *Biochem. J.* **375**, 51-59.

Tremml, G. and Bienz, M. (1989). An essential role of even-skipped for homeotic gene expression in the Drosophila visceral mesoderm. *EMBO J.* **8**, 2687-2693.

Van Doren, M., Mathews, W. R., Samuels, M., Moore, L. A., Broihier, H. T. and Lehmann, R. (2003). fear of intimacy encodes a novel transmembrane protein required for gonad morphogenesis in Drosophila. *Development* **130**, 2355-2364.

Waltzer, L., Vandel, L. and Bienz, M. (2001). Teashirt is required for transcriptional repression mediated by high Wingless levels. *EMBO J.* **20**, 137-145.

Wang, X., Wu, Y. and Zhou, B. (2009). Dietary zinc absorption is mediated by ZnT1 in Drosophila melanogaster. *FASEB J.* **23**, 2650-2661.

Williams, J. A., Bell, J. B. and Carroll, S. B. (1991). Control of Drosophila wing and haltere development by the nuclear vestigial gene product. *Genes Dev.* **5**, 2481-2495.

Yamashita, S., Miyagi, C., Fukada, T., Kagara, N., Che, Y.-S. and Hirano, T. (2004). Zinc transporter LIVI controls epithelial-mesenchymal transition in zebrafish gastrula organizer. *Nature* **429**, 298-302.

SUPPLEMENTAL INFORMATION

A

	genotype	stage	DA1nuclei
A	Control *foi* ^{C887}/*TM3*	16	12.4± 0.4 (n=55)
B	*foi* ^{C887}	16	5.1± 0.5 (n=59)
C	*UASLIV1/+; Mef2Gal4foi*^{C887}*/foi*^{C887}	16	8.5± 0.5 (n=37)
D	*UASCatsup/+; Mef2Gal4foi*^{C887}*/foi*^{C887}	16	6.0± 0.7 (n=35)
E	*UASZip42C/+; Mef2Gal4foi*^{C887}*/foi*^{C887}	16	9.6± 0.8 (n=28)
F	*UASZip71B/+; Mef2Gal4foi*^{C887}*/foi*^{C887}	16	3.8± 0.5 (n=27)
G	*UASZip71B/+; Mef2Gal4foi*^{C887}*/foi*^{C887}(25°)	16	7.8± 0.5 (n=31)
H	*UASZip71B/+; Mef2Gal4foi*^{C887}*/+*	16	4.8± 0.5 (n=41)

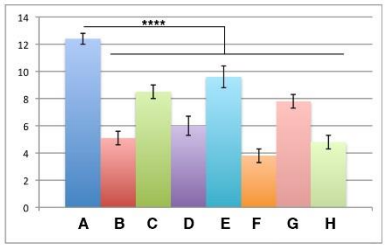

B

	genotype	stage	Twi-nuclei
A	*foi*^{C887}*/TM3*	13	6.3 ± 0.3 (n=10)
B	*foi*^{C887}	13	25.6 ± 2.0 (n=27)
C	*UASfoi;foi*^{C887}	13	18.0 ± 1.8 (n=9)
D	*UASfoi/+; Mef2Gal4foi*^{C887}*/foi*^{C887}	13	7.0 ± 0.5 (n=16)
E	*UASfoi/+; snsGal4foi*^{C887}*/foi*^{C887}	13	8.7 ± 0.9 (n=16)
F	*UASfoi/+; dufGal4foi*^{C887}*/foi*^{C887}	13	13.5 ± 1.3 (n=19)
G	*UASCatsup/+; Mef2Gal4foi*^{C887}*/foi*^{C887}	13	20.0 ± 1.3 (n=9)
H	*UASLIV1/+; Mef2Gal4foi*^{C887}*/foi*^{C887}	13	27.7 ± 2.5 (n=14)
I	*UASZip42C/+; Mef2Gal4foi*^{C887}*/foi*^{C887}	13	6.9 ± 0.4 (n=17)
J	*UASZip71B/+; Mef2Gal4foi*^{C887}*/foi*^{C887}	13	7.3 ± 0.6 (n=15)
K	*Mef2Gal4foi*^{C887}*/UASZnT1foi*^{C887}	13	27.4 ± 1.9 (n=15)
L	*UASminc/+; Mef2Gal4foi*^{C887}*/foi*^{C887}	13	23.8 ± 1.9 (n=31)
M	*minc*^{A388}	13	32.4 ± 1.3 (n=30)

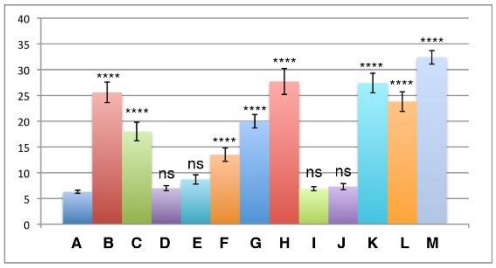

FIGURE S1, related to Figures 3, 6. Quantification of Eve-expressing DA1 nuclei and Twi nuclei in different genetic combinations of *foi*

The figure shows the number of Eve-expressing nuclei in DA1 muscles (A) and Twi-expressing nuclei (B) in embryos at developmental stages 16 (A) or 13 (B) of the indicated genotypes. (*n*, number of hemisegments quantified). Error bars as CI

****P<0.0001 (one-way ANOVA test).

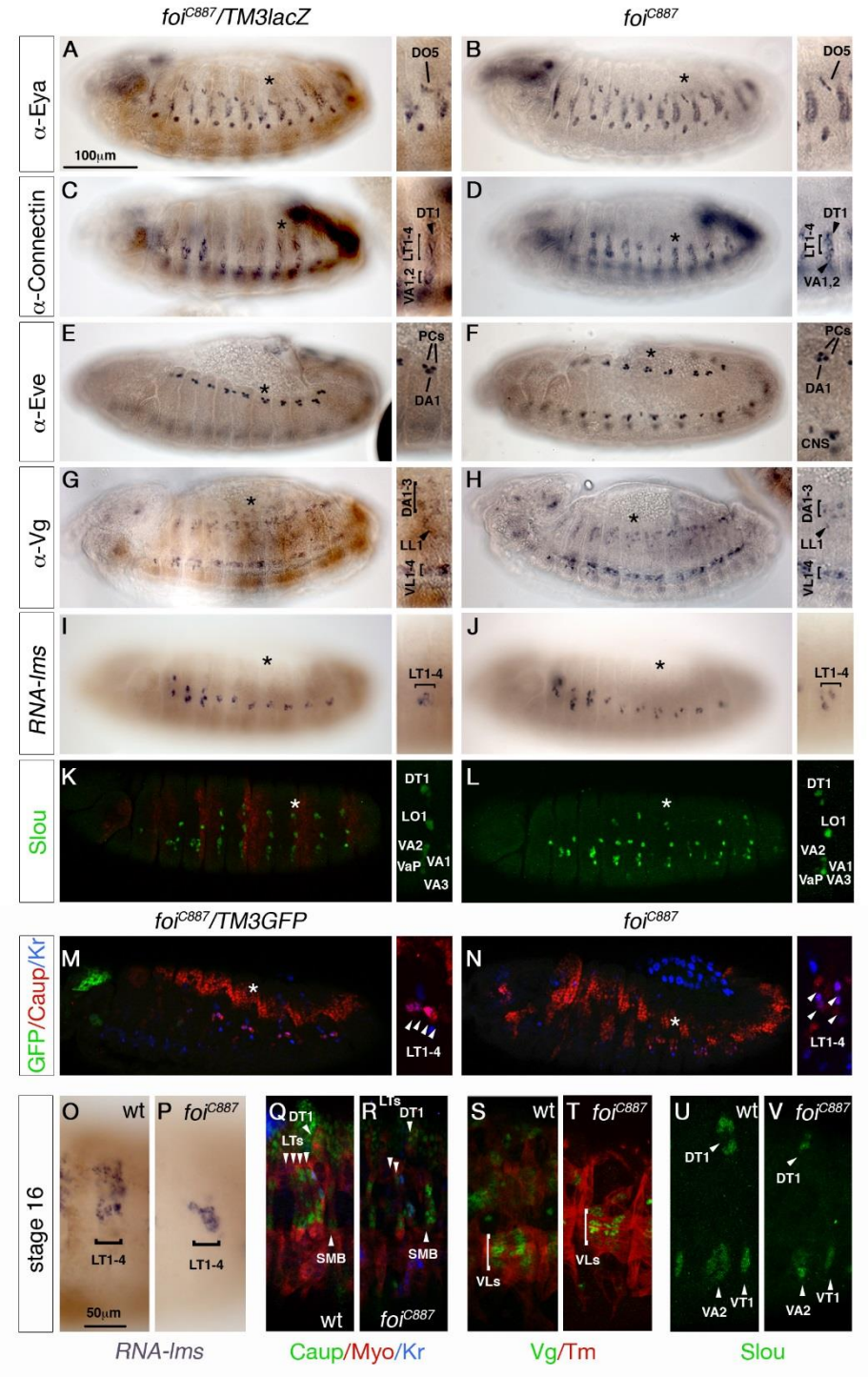

FIGURE S2, related to Figure 2. wild-type and *foi* FCs express the same code of muscle identity genes

(A-N) Lateral views of stage 12-14 control (left column) and *foi* ^{C887} embryos (right column) stained with probe or antibodies for different FC markers as indicated in the

left margin. The magnifications correspond to the hemisegment marked by an asterisk in the corresponding embryo, and show the relevant muscles stained with the different antibodies or probe. Note that the expression of muscle marker genes is initiated properly in *foi* mutants although muscles contain fewer nuclei due to the fusion defect. (O-V) Details of the lateral regions of stage 16 control and *foi* mutant embryos stained with probe or antibodies for FC markers as indicated. The confocal images show Z projections of several consecutive sections.

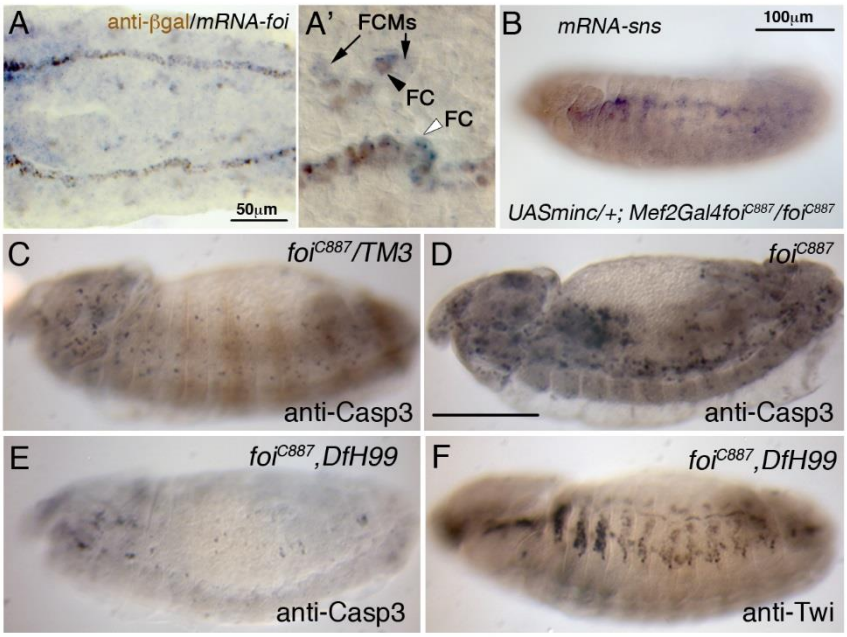

FIGURE S3, related to Figures 2, 3. The blockade of myogenic differentiation in *foi* FCMs causes their elimination by apoptosis

(A, A') ventral view of a *rP298* stage 11 embryo showing that *foi* transcripts accumulate in somatic and visceral founders (FC, black and white arrowheads in A') and in fusion-competent myoblasts (FCMs, arrows in A'). (B) Over-expression of *minc* in the mesoderm of *foi* embryos cannot restore *sns* expression. (C-E) Lateral views of stage 14 control (C), *foi*^{C887} (D) and *foi*^{C887} *DfH99* (E) embryos stained with an antibody to activated Caspase 3. Note the large number of apoptotic FCMs in *foi* ^{C887} embryos that are not seen in *foi* ^{C887} *DfH99*. (F) Lateral view of a stage 14 *foi*^{C887} *DfH99* embryo stained with anti-Twist to show the faulty differentiation of FCMs.

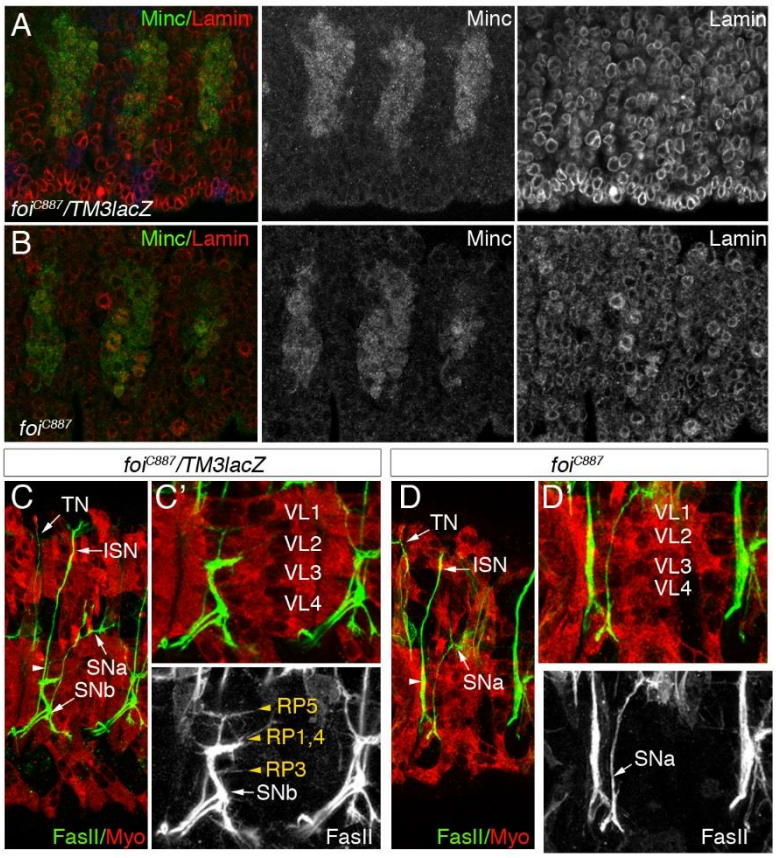

FIGURE S4, related to Figure 2. Minc subcellular localization and innervation defects in *foi* mutants

(A, B) Lateral views of three abdominal segments of stage 14 control (*foi*^{C887}*/TM3lacZ*, A) and *foi*^{C887} (B) embryos stained with antibodies against Minc (green) and Lamin (Red) to label the nuclear membrane. In both genotypes Minc protein is found in the nuclei and cytoplasm. (C-D') Ventro-lateral regions of control (*foi*^{C887}*/TM3lacZ*, C) and *foi*^{C887} (D) late stage 16 embryos stained with anti Myosin (red) and anti-FasII (green) to reveal the peripheral motor projections. In *foi* mutants the SNb branch does not defasciculate from the dorsal ISN leaving ventral muscles without innervation. Note the thickening of the ISN in D (arrowhead, compare to C).

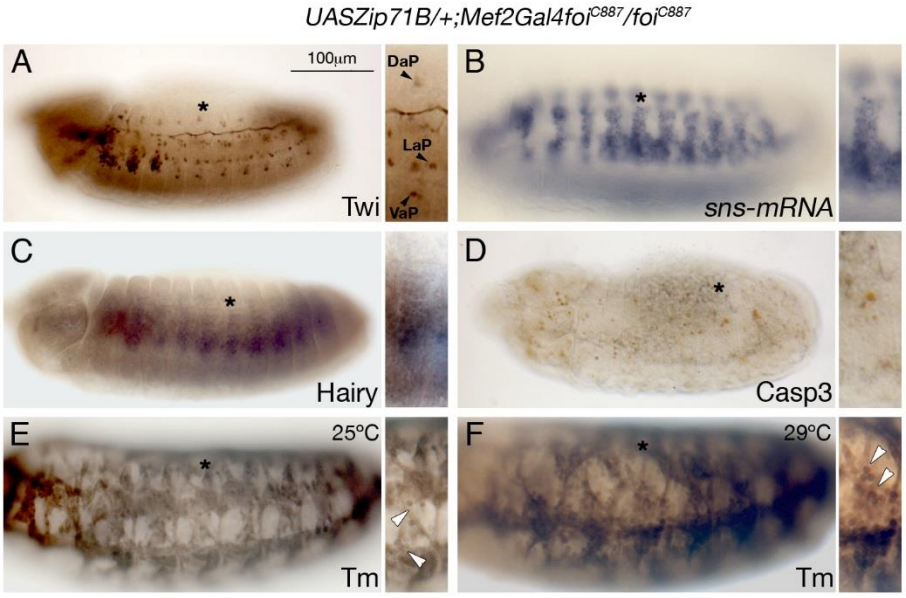

FIGURE S5, related to Figure 6. Mesodermal rescues of *foi* phenotypes with *Zip71B*

(A-F) Stages 13 (D), 14 (A-C) and 16 (E, F) *foi*^{C887} embryos with panmesodermal expression of the zinc transporter *Zip71B*. *Zip71B* causes a substantial rescue of *foi* mesodermal phenotypes as evidenced by Twi (A), *sns-mRNA* (B) and Hairy (C) patterns of expression. These conditions of *Zip71B* mesodermal expression result in a weak non fusion phenotype, as seen by the presence of unfused myoblasts at stage 16 (arrowheads in E inset), that is aggravated with the increase of temperature (arrowheads in F inset) without inducing a significant death of myoblasts (D).